

# SIMULATION OF ION-TEMPERATURE-GRADIENT TURBULENCE IN TOKAMAKS<sup>1</sup>

A.M. DIMITS, B.I. COHEN, N. MATTOR, W.M. NEVINS,  
D.E. SHUMAKER  
Lawrence Livermore National Laboratory  
Livermore, CA 94551  
USA

S.E. PARKER, C. KIM  
University of Colorado  
Boulder, CO 80309  
USA

## Abstract

Results are presented from nonlinear gyrokinetic simulations of toroidal ion temperature gradient (ITG) turbulence and transport. The ion thermal *fluxes* are found to have an offset linear dependence on the temperature gradient and are significantly lower than gyrofluid or IFS-PPPL-model predictions. A new phenomenon of nonlinear effective critical gradients larger than the linear instability threshold gradients is observed, and is associated with undamped flux-surface-averaged shear flows. The nonlinear gyrokinetic codes have passed extensive tests which include comparison against independent linear calculations, a series of nonlinear convergence tests, and a comparison between two independent nonlinear gyrokinetic codes. Our most realistic simulations to date used actual reconstructed equilibria from experiments and a model for dilution by impurity and beam ions. These simulations highlight the importance of both self-generated and “external  $\mathbf{E} \times \mathbf{B}$  flow shear as well as the need for still more physics to be included.

## 1. INTRODUCTION

The results of nonlinear  $\delta f$ -particle gyrokinetic simulations of toroidal ion-temperature-gradient (ITG) turbulence are reported here. This work is motivated by the need to develop models of anomalous transport of heat, particles, and momentum in tokamaks and other magnetic plasma confinement devices [1]. Toroidal ITG turbulence is considered to be a likely mechanism to explain momentum and ion thermal transport, however the quantitative picture is still incomplete.

Tremendous advances in simulation algorithms and computer power, as well as targeted investments in code development have made nonlinear  $\delta f$  gyrokinetic simulation a practical tool for studying ITG and other (e.g., trapped-electron) microturbulence for realistic plasma parameter values. This provides opportunities for better characterization of the turbulent transport and for the discovery of qualitatively new behavior, both because of the very large ( $> 7$ -dimensional) parameter space and because of the limitations of the various reduced treatments of the kinetic processes on which much of the present understanding is based.

The IFS-PPPL model [2] has attracted attention because of its success in interpreting some plasmas. This model combines nonlinear gyrofluid and quasilinear gyrokinetic calculations into a single transport model. The nonlinear gyrofluid models are supposed to be approximations to the gyrokinetic equations. However, we find that for some relevant experimental conditions, gyrokinetic simulations give a value of the thermal diffusivity  $\chi_i$  roughly a factor of 3 lower than that given by gyrofluid simulations and the IFS-PPPL model. Such differences may have a significant impact on predictions of tokamak (e.g., ITER) plasma performance. It is therefore

---

<sup>1</sup>This work was performed by LLNL for USDoe under contract W-7405-ENG-48, and is part of the US NTTP and Cyclone projects.

of great importance and interest to establish the validity of the gyrokinetic results.

## 2. GYROKINETIC SIMULATION CODES AND NUMERICAL PARAMETERS

This paper discusses results from two independent nonlinear gyrokinetic codes (LLNL [3] and U. Colorado, Boulder [4]) which incorporate the advances mentioned above, including  $\delta f$  algorithms [5, 6], field aligned numerical representation [7], and flux-tube simulation domains [8, 9]. The codes are toroidal, nonlinear, and electrostatic, and have fully toroidal nonlinear gyrokinetic ions [10] with equilibrium temperature and density gradients. The gyrokinetic Vlasov equation is solved using the partially linearized  $\delta f$  particle method [5, 6]. The electron response is taken to be adiabatic, with a zero response to the flux-surface-averaged potential  $\langle \phi \rangle_{\theta, \phi}$  [11]. Self-generated turbulent-Reynolds'-stress-driven flows are included fully. The simulation domain used is a flux tube which spans one or more poloidal circuits in the parallel direction. Profile relaxation is prevented by making the simulation volume seamlessly periodic, with a “twist-shift” radial periodicity condition [6] and parallel periodicity consistent with the mode physics.

Typical values of the timestep  $dt$ , grid sizes respectively in the radial, toroidal (perpendicular), and parallel directions,  $\Delta_x$ ,  $\Delta_y$  and  $\Delta_z$ , and the respective numbers of grid cells  $N_x$ ,  $N_y$ , and  $N_z$  are given by  $dt c_s / L_T = 0.2$ , where  $c_s \equiv \sqrt{T_e / m_i}$ ,  $T_e$  is the electron temperature,  $m_i$  is the ion mass,  $L_T$  is the ion temperature gradient scale length,  $\Delta_x / \rho_s = \Delta_y / \rho_s = 0.8\text{--}1.0$ , where  $\rho_s = c_s / \Omega_i$ , and  $\Omega_i$  is the ion gyrofrequency,  $\Delta_z = 2\pi q R / N_z$ , where  $q \equiv r B_t / R B_p$  is the magnetic “safety factor,”  $R$  and  $r$  are respectively the major and minor radii, and  $B_t$  and  $B_p$  are the toroidal and poloidal magnetic field components,  $N_x = N_y = 128$ , and  $N_z = 32\text{--}64$ . At least 16 particles per grid cell were used in the LLNL gyrokinetic code, except in the case of the particle number scan results shown in Sect. 4 where the particle numbers are given explicitly, and 8 particles per cell in the U. Col. Boulder runs shown in Sect. 3.

The thermal diffusivity is defined formally as

$$\chi_i = 1.5 L_T \langle \tilde{V}_x \tilde{T}_i \rangle / T_i, \quad (1)$$

where  $\tilde{V}_x$  and  $\tilde{T}_i$  are the fluctuating components of the radial ion velocity and temperature and  $T_i$  is the equilibrium ion temperature. In practice,  $\chi_i$  is calculated as a suitable weighted sum over the simulation particles. For sufficiently large box sizes  $\chi_i / \chi_{GB}$ , where  $\chi_{GB} \equiv \rho_s^2 c_s / L_T$ , is finite and independent of the box size, irrespective of the magnetic shear [3]. The transport therefore has a clear gyroBohm scaling.

## 3. TEMPERATURE GRADIENT SCANS

Figure 1 shows the predictions for  $\chi_i$  vs.  $R / L_T$ , for a scan about the “Cyclone DIII-D base case” parameters. This parameter set represents local parameters from an ITER-relevant DIII-D plasma [12], shot #81499, at time  $t = 4000\text{ms.}$ , and  $r/a = 0.5$ , where  $a$  is the minor radius of the separatrix. The parameter values, in dimensionless form are  $\eta_i \equiv L_n / L_T = 3.114$ , where  $L_n$  is the the density gradient scale length,  $q = 1.4$ ,  $\hat{s} \equiv (r/q) dq/dr = 0.78$ ,  $R/L_T = 6.92$ , and  $\epsilon_B \equiv r/R = 0.18$ . These simulations used circular cross-section model equilibria and a single dynamical (bulk) ion species, as did the nonlinear gyrofluid simulations that underly the IFS-PPPL model.

Shown are the results from our (LLNL and U. Col. Boulder) gyrokinetic simulations and from the IFS-PPPL model, as well as a similar (LLNL-gyrokinetic-code) scan with  $\epsilon_B = 0$ . A remarkably good fit to the dependence of the *thermal flux* from the LLNL gyrokinetic simulations on the temperature gradient for this scan can be obtained by an offset linear dependence on  $R/L_T$ . In terms of  $\chi_i$ , this fit can be expressed as

$$\chi_i L_n / (\rho_i v_{ti}^2) \simeq 15.4 [1.0 - 6.0 (L_T / R)], \quad (2)$$

and is shown as the dot-dashed line on Fig. 1. The simplicity and quality of such a fit are

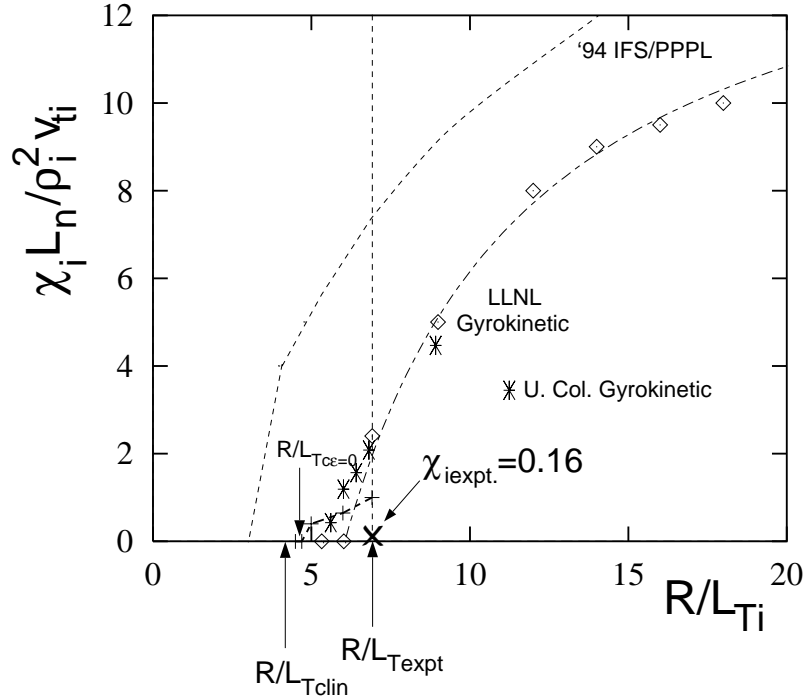


Figure 1: Normalized  $\chi_i$  vs  $R/L_{Ti}$  from gyrokinetic simulations, and '94 IFS-PPPL model.

highly suggestive, and it would be of great interest to explore whether such a fit works for other temperature-gradient scans.

For the base parameter value  $R/L_T = 6.92$ , the gyrokinetic  $\chi_i$  is about a factor of 3 lower than that give by the IFS-PPPL-model, which is a somewhat larger difference than was observed for the TFTR “NTP test case” [3]. The relative disagreement between the gyrokinetic results and the IFS-PPPL formula is largest for small values of  $R/L_T$ , and generally decreases as  $R/L_T$  increases. The disagreement can be characterized roughly as a shift in  $R/L_T$  of the  $\chi_i$  vs.  $R/L_T$  curves, and not as a simple multiplicative factor in  $\chi_i$ . Beer [13] has verified that for this parameter scan, nonlinear gyrofluid simulations agree reasonably well with the IFS-PPPL model (within 27% for  $R/L_T = 4.0$ – $9.0$ ).

#### 4. LINEAR TESTS

In order to establish confidence in the gyrokinetic simulation results, both linear benchmarks and and nonlinear tests have been undertaken.

The linear ITG-mode frequencies and growth rates and critical temperature gradients obtained from the LLNL gyrokinetic code have been compared found to agree very well with independent linear codes [13], both for the Cyclone base case and for a case with the same local parameters, except  $\epsilon_B = 0$ .

A second linear test is against a theory due to Rosenbluth and Hinton [14] for the residual levels of purely “radial” modes of the electrostatic potential (i.e., modes which have no variation within a flux surface and which represents a near poloidal  $\mathbf{E} \times \mathbf{B}$  flows) in the collisionless limit. Here, the gyrokinetic code is initialized with zero  $\delta f$  particle weights. A radially sinusoidal potential with no variation within the flux surfaces is imposed. The particle weights evolve, resulting in geodesic acoustic oscillations, which damp through linear processes, and a nonzero undamped residual. In the large aspect-ratio limit, the theoretical prediction for the ratio of the late-time residual potential to the initial potential is given as a function  $0.6h/(1.0 + 0.6h)$  of the single parameter  $h \equiv \sqrt{\epsilon_B}/q^2$  [14].

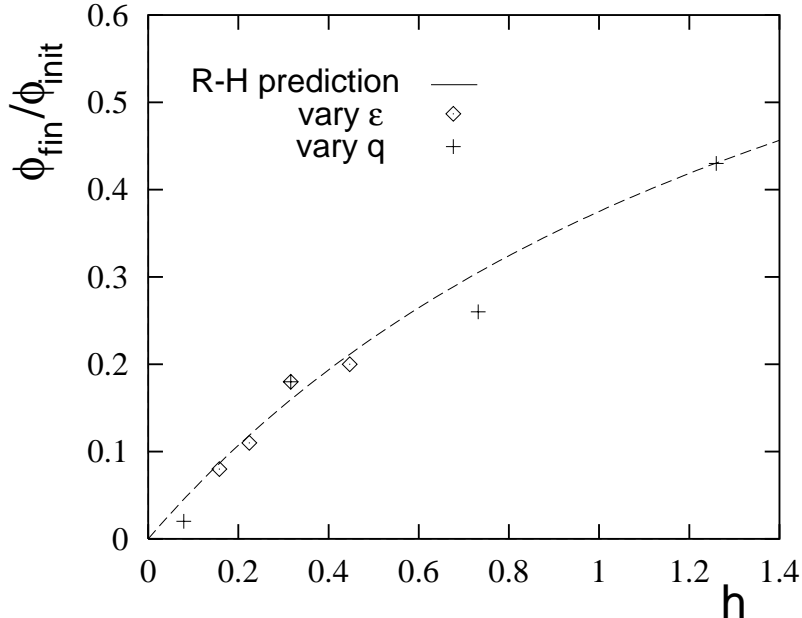


Figure 2: *Residual flux-surface-averaged flow fraction vs. Rosenbluth-Hinton parameter  $h \equiv \sqrt{\epsilon_B}/q^2$ . The points are gyrokinetic code results and the line is prediction of Ref. [14].*

Figure 2 shows the fractional residual  $\mathbf{E} \times \mathbf{B}$  flows for two scans (varying  $q$  and  $\epsilon_B$  respectively) using the LLNL gyrokinetic code, along with the prediction of Ref. [14]. Very good agreement is observed, giving confidence to both the RH theory and the simulation.

## 5. EFFECTIVE NONLINEAR CRITICAL GRADIENT

A new result from the gyrokinetic simulations, evident in Fig. 1, is that there is a range of values of the normalized temperature gradient  $R/L_T$ , between the linear critical gradient  $R/L_{T\text{crit}}$  and an effective nonlinear critical gradient  $R/L_{T\text{eff}}$  in which the simulations are linearly unstable, but for which the thermal transport at late time becomes essentially zero. This phenomenon appears to be associated with undamped  $\mathbf{E} \times \mathbf{B}$  flows predicted by Rosenbluth and Hinton [14]. A large, very steady flux-surface-averaged potential  $\langle \phi \rangle_{\theta, \phi}$  is observed in the cases with  $R/L_{T\text{crit}} < R/L_T < R/L_{T\text{eff}}$ . In contrast, for cases with  $R/L_T > R/L_{T\text{eff}}$ , the profiles of  $\langle \phi \rangle_{\theta, \phi}$  move as time evolves. The peak shearing rates associated with  $\langle \phi \rangle_{\theta, \phi}$  are of order three times the growth rate of the fastest growing ITG modes.

In the  $\epsilon_B = 0$  gyrokinetic simulation scan shown in Fig. 1, there is no discernible separation between  $R/L_{T\text{eff}}$  and  $R/L_{T\text{crit}}$ . This is to be expected if the undamped Rosenbluth-Hinton flows play a key role in the departure of  $R/L_{T\text{eff}}$  from  $R/L_{T\text{crit}}$ , since the residual flow fraction goes to zero as  $\epsilon_B$  goes to zero.

## 6. NUMERICAL CONVERGENCE

Next, we examine whether the gyrokinetic simulations are converged with respect to particle number. Fig. 3 shows  $\chi_i$  vs. time from a particle number scan. The simulations are for different numbers of particles ranging from  $5 \times 10^5$  to  $1.34 \times 10^8$ . For  $10^6$  or more particles (2 particles per cell),  $\chi_i$  at late time does not appear change with increasing particle number. Thus,  $\chi_i$  appears to be well converged wrt. particle number for more than 2–4 particles per cell.

There is some random variation in the late time-averaged  $\chi_i$  for the different cases, but this is

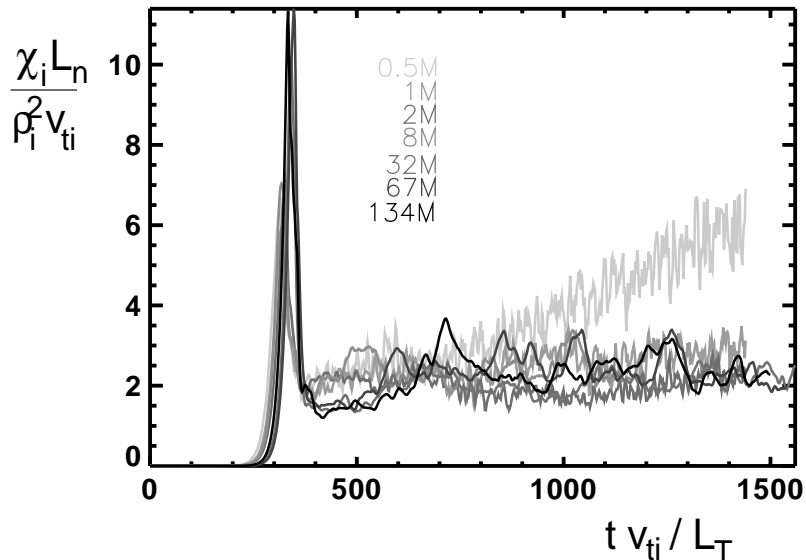


Figure 3: Normalized  $\chi_i$  vs.  $tv_{ti}/L_T$  from gyrokinetic simulations with particle numbers ranging from  $5 \times 10^5$  to  $1.34 \times 10^8$ .

small, and has no systematic dependence on particle number. There is also some increase in the level of the initial peak with particle number, which persists even if the scan is done increasing the initial weights (as the square root of the particle number) so as to keep the initial mean noise level fixed. The  $5 \times 10^5$ -particle case shows secular growth in  $\chi_i$  beyond  $tv_{ti}/L_T = 700$ . This is due to a noise-driven runaway process in which the detailed  $\delta f$ -particle entropy, most of which is due to noise, increases with the time integral of  $\chi_i$ . The noise causes thermal transport ( $\chi_i$ ), both of which increase together.

In order to further assess the impact of particle discreteness, the following “scrambling test” [15] of the noise level was performed. The gyrokinetic code was run using Cyclone base case parameters, for  $8 \times 10^6$  and  $1.6 \times 10^7$  particles, and restart files were saved at selected times. New restart files were formed from these by scrambling the particle  $\delta f$  weight list [5, 6]. The gyrokinetic code was restarted from these scrambled restart files. The scrambled restart eliminates the physical signal but leaves fluctuations whose level is a measure of the noise in the simulation due to particle discreteness. After the restart, the temperature gradient was reduced to slightly below the linear marginally stable value in order to eliminate unstable ITG modes, but to still allow measurement of (noise-driven) diffusion through a transport flux. Shown in Fig. 4 is the time histories of  $\chi_i$ , both in the absence of scrambling and when the scrambling and gradient reduction is done at three times during the run.  $\chi_i$  is reduced after the scrambling. The relative reduction is less the later the scrambling is done, indicating a gradual buildup of noise. However, even at the latest time, the post scrambling values are down by an order of magnitude. Thus, the relative impact of noise is small, supporting the conclusion that the simulations are converged with respect to particle number.

An exception has been observed for cases with  $R/L_{Tcrit} < R/L_T < R/L_{Teff}$  (see Sect. 4). It is found that  $R/L_{Teff}$  increases slowly with particle number, so that for the Cyclone base case  $R/L_T$  scan, for example,  $R/L_{Teff} > 6.0$ , but at least  $\sim 64$  particles per cell are needed for an  $R/L_T = 6.0$  case to yield zero  $\chi_i$ .

We have also completed simulations in which the parallel and perpendicular system sizes

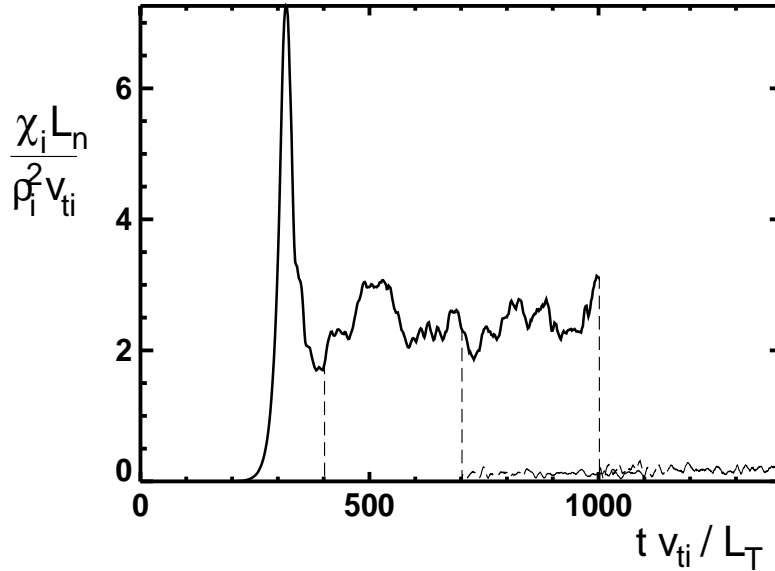


Figure 4: Normalized  $\chi_i$  vs. time from Cyclone DIII-D base case and three scrambled restarts.

were increased by a factor of 2 over the nominal values given in Sect. 2 (keeping the grid sizes and number of particles per grid cell fixed), as well as simulations in which the grid sizes were reduced by a factor of 2 (keeping system size and the number of particles per grid cell, and grid filter size divided by grid size fixed). In all cases,  $\chi_i$  was unaltered from the corresponding case using the nominal numerical parameter values, which demonstrates that these nominal system and grid sizes are adequate.

## 7. SIMULATIONS USING REALISTIC EXPERIMENTAL EQUILIBRIA

The LLNL gyrokinetic code has been extended to use realistic equilibria, obtained by direct reconstruction from experimental data, as well as a dilution model for the effects of impurity and beam ion species. Figure 5 shows the  $\chi_i$  vs. normalized minor radius  $\rho$  from such simulations for DIII-D shot #84736 at  $t=1200$ ms. This shot is a high-performance negative-central-shear (“NCS”) L-mode plasma with an internal transport barrier. The simulations show order-of-magnitude agreement with the experiment, but the wrong trend with minor radius. Several additional physics effects are expected to produce order-one changes in  $\chi_i$ , including nonadiabatic electrons, active impurity dynamics, collisions, velocity shear, and radial profile variation.

Shown in Fig. 5 is a simulation result, at  $\rho = 0.3$ , in which the equilibrium scale perpendicular and parallel velocity shear components inferred from the experimental data were included. This reduced the turbulent  $\chi_i$  to zero, in agreement with the observation that at  $\rho = 0.3$ , the transport is neoclassical.

## 8. EQUILIBRIUM-PROFILE-SCALE EFFECTS

Radial variations in the equilibrium temperature gradient have been implemented in the LLNL gyrokinetic code and their effects examined. Studies using global gyrokinetic codes suggest that this is potentially the most important profile-scale effect. Simulation runs were completed using the Cyclone base case parameters, but with temperature gradient profiles of the form  $L_T^{-1} = L_{T0}^{-1}[1 + \delta \cos 2\pi(r - r_0)/\Delta_x]$ , with  $\Delta_x = 125\rho_i$ , and  $\delta = 1/3$ . For  $R/L_{T0} = 5.19$ , so

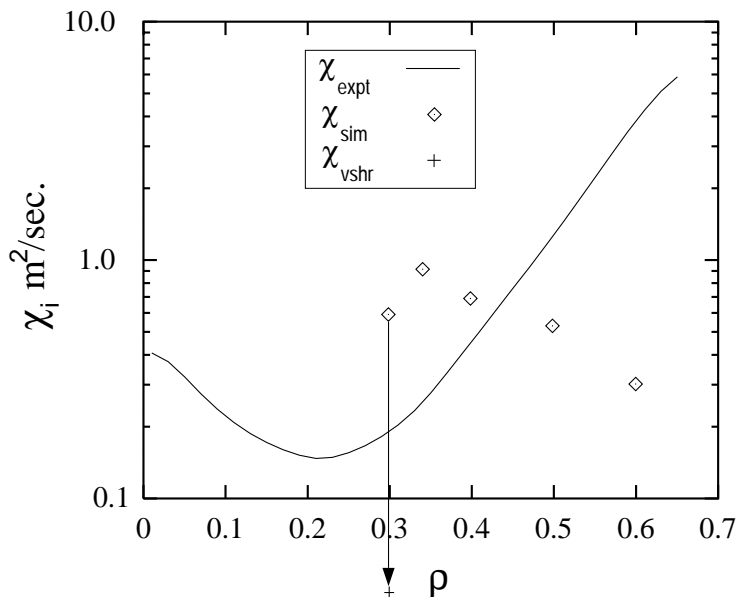


Figure 5:  $\chi_i$  vs. normalized minor radius from gyrokinetic simulations of DIII-D shot 84736,  $t=4000$ ms. The runs had zero external velocity shear, except the one indicated by the arrow.

that the peak temperature gradient is as for the Cyclone base case (roughly characteristic of the experimental profile),  $\chi_i$  is greatly reduced and approaches zero at late time. For  $R/L_{T0} = 6.92$  and 12.0 respectively, the reduction in  $\chi_i$  compared to the corresponding  $\delta = 0$  cases are of order 40% and 10%.

A new way to obtain more detailed information is by examination of scatter (or correlation) plots of the time-averaged local thermal flux vs. the time-averaged net temperature gradient using data from the nonlinearly saturated phase of the simulations. We observe that in such scatter plots from a single simulation run, there is considerable scatter both in gradient and flux, and no tendency for the points to cluster along the curve obtained from the uniform-initial-gradient simulations (shown in Fig. 1). There are points with gradients significantly higher than the average and fluxes lower, and vice versa. Thus the sub regions of these simulations do not behave locally.

## 9. SUMMARY AND CONCLUSIONS

In this work, the temperature-gradient dependence of ITG turbulent transport was studied. The gyrokinetic simulations are found to yield ion thermal fluxes which have an offset linear dependence on the temperature gradient and which are significantly lower than gyrofluid or IFS-PPPL-model predictions. The existence of an effective critical temperature gradient greater than the linear critical value has been observed, and correlates well with the presence of undamped flux-surface-averaged  $\mathbf{E} \times \mathbf{B}$  flows predicted in Ref. [14]. Several linear and nonlinear tests and comparisons have been completed which strongly support the validity and viability of gyrokinetic simulations. Profile-scale velocity shear and temperature-gradient variation over realistic spatial scales were shown to be important.

Some simulation results using realistic equilibria were presented. While there has been much progress on including many important physical effects in the gyrokinetic codes, more is needed. Nonadiabatic electrons, collision models, and dynamically active impurity species are all important and need to be included as self-consistently as possible. Having established

considerable confidence in the nonlinear gyrokinetic codes, attention is being devoted to these important physics enhancements.

## ACKNOWLEDGMENTS

The simulations were done on the NERSC T3E. We thank C. Bolton for his encouragement and support, as well other Cyclone participants, especially M. Beer, W. Dorland, G. Hammett, M. Kotschenreuther for fruitful discussions. This work was performed under the auspices of U.S. Department of Energy (DoE) by Lawrence Livermore National Laboratory under contract No. W-7405-ENG-48, and is part of the Numerical Tokamak Turbulence Project supported by the High Performance Computing and Communications Program in the U.S. DoE, as well as the DoE-OFE Cyclone Initiative.

## References

- [1] see, for example, T.C. Luce *et al.*, in *Proc. 15th. Int. Conf. on Plasma Physics and Controlled Nuclear Fusion* (1995, IAEA), paper A-2-III-2.
- [2] W. Dorland, M. Kotschenreuther, M.A. Beer, G.W. Hammett, R.E. Waltz, R.R. Dominguez, P.M. Valanju, W.H. Miner, J.Q. Dong, W. Horton, F.L. Waelbroeck, T. Tajima, and M.J. LeBrun, in *Plasma Physics and Controlled Nuclear Fusion Research, 1994*, paper IAEA-CN-60/D-P-I-6.
- [3] A.M. Dimits *et al.*, PRL **77**, 71 (1996).
- [4] S.E. Parker, W. Dorland, R.A. Santoro, M.A. Beer, Q.P. Liu, W.W. Lee, and G.W. Hammett, Phys. Plasmas **1**, 1461 (1994).
- [5] A. M. Dimits, Ph.D. thesis, Princeton University, Feb. 1988; A. M. Dimits and W. W. Lee, J. Comp. Phys. **107**, 309 (1993).
- [6] M. Kotschenreuther *et al.*, in *Proc. 14th. Int. Conf. on Plasma Physics and Controlled Nuclear Fusion, 1992* (1993, IAEA, Vienna), Vol. 2, 11.
- [7] A. M. Dimits, Phys. Rev. E**48**, 4070 (1993).
- [8] P.N. Guzdar, J.F. Drake, D. McCarthy, A.B. Hassam, and C.S. Liu, Phys. Fluids B**5**, 3712 (1993).
- [9] M.A. Beer, S.C. Cowley, and G. W. Hammett, Phys. Plasmas **2**, 2687 (1995).
- [10] E. A. Frieman and Liu Chen, Phys. Fluids **25**, 502 (1982).
- [11] B.I. Cohen, T.J. Williams, A.M. Dimits and J.A. Byers, Phys. Fluids B**5**, 2967 (1993).
- [12] C.M. Greenfield, J.C. DeBoo, T.H. Osborne, F.W. Perkins, M.N. Rosenbluth, D. Boucher, Nuclear Fusion **37**, 1215 (1997).
- [13] M.A. Beer (1997, private communication).
- [14] M.N. Rosenbluth and F.L. Hinton, PRL **80**, 724 (1998).
- [15] The scrambling noise test was proposed originally by M. Kotschenreuther, and valuable variations and refinements were suggested by W. Dorland, G.W. Hammett, and M.N. Rosenbluth in private communications dating between 1995 and 1997.